Published in final edited form as:
J Cell Physiol. 2008 December ; 217(3): 674–685. doi:10.1002/jcp.21537.

Induction of HIF-1α Expression by Intermittent Hypoxia: Involvement of NADPH Oxidase, Ca^{2+} Signaling, Prolyl Hydroxylases, and mTOR

Guoxiang Yuan[1], **Jayasri Nanduri**[1], **Shakil Khan**[1], **Gregg L. Semenza**[2], and **Nanduri R. Prabhakar**[1,*]

[1] The Center for Systems Biology, Department of Medicine, University of Chicago, IL 60637, USA

[2] Vascular Program, Institute for Cell Engineering and Departments of Pediatrics, Medicine, Oncology, Radiation Oncology, and McKusick-Nathans Institute of Genetic Medicine, The Johns Hopkins University School of Medicine, Baltimore, MD, 21205, USA

Abstract

Sleep-disordered breathing with recurrent apnea (periodic cessation of breathing) results in chronic intermittent hypoxia (IH), which leads to cardiovascular and respiratory pathology. Molecular mechanisms underlying IH-evoked cardio-respiratory co-morbidities have not been delineated. Mice with heterozygous deficiency of hypoxia-inducible factor 1α (HIF-1α) do not develop cardio-respiratory responses to chronic IH. HIF-1α protein expression and HIF-1 transcriptional activity are induced by IH in PC12 cells. In the present study, we investigated the signaling pathways associated with IH-evoked HIF-1α accumulation. PC12 cells were exposed to aerobic conditions (20% O_2) or 60 cycles of IH (30 sec at 1.5% O_2 followed by 5 min at 20% O_2). Our results show that IH-induced HIF-1α accumulation is due to increased generation of ROS by NADPH oxidase. We further demonstrate that ROS-dependent Ca^{2+} signaling pathways involving phospholipase Cγ and protein kinase C activation are required for IH-evoked HIF-1α accumulation. IH leads to activation of mTOR and S6 kinase and rapamycin partially inhibited IH-induced HIF-1α accumulation. IH also decreased hydroxylation of HIF-1α protein and anti-oxidants as well as inhibitors of Ca^{+2} signaling prevented this response. Thus, both increased mTOR-dependent HIF-1α synthesis and decreased hydroxylase-dependent HIF-1α degradation contribute to IH-evoked HIF-1α accumulation. Following IH, HIF-1α and phosphorylated mTOR levels remained elevated during 90 min of re-oxygenation despite re-activation of prolyl hydroxylase. Rapamycin or cycloheximide, blocked increased HIF-1α levels during re-oxygenation indicating that mTOR-dependent protein synthesis is required for the persistent elevation of HIF-1α levels during re-oxygenation.

Keywords

Intermittent hypoxia; HIF-1α; NADPH oxidase; Calcium signaling; Prolyl hydroxylases; mTOR

Introduction

Breathing disorders with recurrent apnea (cessation of breathing) during sleep result in periodic decreases in arterial blood PO_2 or chronic intermittent hypoxia (CIH). In severely affected subjects, O_2 saturation of arterial blood hemoglobin can be reduced to as low as

*Correspondence to: Nanduri R. Prabhakar, Center for Systems Biology, Department of Medicine, MC 5068, 5841 South Maryland Avenue, Chicago, IL 60637. USA. Tel: 773-834-5480, Fax: 773-834-5252, E-mail: nanduri@uchicago.edu.

50%. Recurrent sleep apnea affects an estimated 4–5% of adult males, 2–4% of females after menopause, and 50–70% of premature infants (Nieto et al., 2000; Poets et al., 1994). Co-morbidities associated with CIH include pulmonary as well as systemic hypertension, myocardial infarction, stroke, ventilatory abnormalities, and sudden death in elderly individuals (Shahar et al., 2001). Clinical and animal studies have shown that reflexes arising from the carotid body, which senses arterial PO_2, play a critical role in CIH-evoked autonomic abnormalities (reviewed in Prabhakar et al., 2007a). Little information, however, is available on the cellular and molecular mechanisms associated with CIH.

The transcriptional activator hypoxia inducible factor 1 (HIF-1) is a global regulator of oxygen homeostasis that controls hundreds of target genes, including those encoding erythropoietin (*EPO*), vascular endothelial growth factor (*VEGF*) and proteins associated with glucose and energy metabolism (Semenza, 2007). HIF-1 is a heterodimeric protein that is composed of a constitutively expressed HIF-1β subunit and an O_2-regulated HIF-1α subunit. HIF-1 activity is induced under conditions of continuous hypoxia as a result of a decreased rate of O_2-dependent proline hydroxylation, ubiquitination, and proteasomal degradation of the HIF-1α subunit (Coleman and Ratcliffe, 2007). HIF-1α transcriptional activity is also regulated via O_2-dependent asparagine hydroxylation that blocks co-activator recruitment (Peet, 2004).

Complete HIF-1α deficiency results in embryonic lethality at mid-gestation, whereas *Hif1a*$^{+/-}$ heterozygous mice, which are partially deficient in HIF-1α expression, develop normally and are indistinguishable from wild type littermates under normoxic conditions (Iyer et al., 1998; Yu et al., 1999). However, carotid body responses to continuous hypoxia (CH) are selectively impaired in adult *Hif1a*$^{+/-}$ mice, indicating that HIF-1 plays an essential role in O_2 sensing/signaling by the carotid body (Kline et al., 2002). Peng et al (2006) reported that in wild type mice, CIH markedly affects the cardio-respiratory systems resulting in: augmented hypoxic ventilatory response; long-term facilitation (LTF) of breathing; enhanced carotid body response to graded hypoxia and sensory LTF; increased arterial blood pressures; and elevated plasma norepinephrine levels. In striking contrast, in *Hif1a*$^{+/-}$ mice exposed to CIH, carotid body responses to acute IH, as well as all measured cardio-respiratory responses, were either absent or markedly attenuated (Peng et al., 2006). These observations suggest a critical role for HIF-1 in mediating the cardio-respiratory changes that are induced by CIH. In humans, genetic defects that dysregulate HIF-1 activity, have profound effects on erythropoiesis and ventilation (Ang et al., 2002; Smith et al., 2006). Given its pathophysiological significance, it is of considerable importance to delineate the mechanisms that induce HIF-1 activity in response to CIH.

The rat pheochromocytoma PC12 cell line shares a number of characteristics with the oxygen-sensing type I (glomus) cells in the carotid body (Peers, 2004). Yuan et al (2005) reported that exposure of PC12 cells to IH led to increased HIF-1α protein expression and transactivation, resulting in increased HIF-1-dependent gene transcription. IH-induced HIF-1 transactivation requires Ca^{2+}/calmodulin kinase (CaMK)-dependent phosphorylation of the co-activator p300, which appears to increase its interaction with HIF-1α under non-hypoxic conditions, when asparagine hydroxylation of HIF-1α would otherwise prevent their interaction (Yuan et al., 2005). CIH leads to robust and sustained CaMK activation in PC12 cells (Yuan et al., 2005). In striking contrast, exposure of PC12 cells to continuous hypoxia (CH) results in a transient and modest activation of CaMK (Premkumar et al., 2000). Although both IH and CH induce tyrosine hydroxylase, a downstream HIF-1 regulated gene, only IH-induced tyrosine hydroxylase expression was blocked by KN93, a selective inhibitor of CaMK (Yuan et al., 2005). These observations demonstrate that HIF-1 activity is induced by different mechanisms in cells exposed to CH as opposed to IH. Most importantly, KN93 blocked the increase in HIF-1 transcriptional activity but not the increase

in HIF-1α protein expression in response to IH, indicating that CaMK-independent and CaMK-dependent pathways mediate IH-induced HIF-1α protein expression and transactivation, respectively (Yuan et al., 2005).

Recent studies on animal models (Peng et al., 2003; Yuan et al., 2004; Kumar et al., 2006; Ramanathan et al., 2005) suggest that CIH increases reactive oxygen species (ROS). Increased generation of ROS was also reported in recurrent apnea patients experiencing CIH and antioxidants prevent systemic and cellular responses to CIH (reviewed in Prabhakar et al., 2007b). In CIH exposed mice, HIF-1α protein levels increased in the central nervous system and anti-oxidants prevented this response (Peng et al., 2006). In the present study, we have delineated a complex signal transduction cascade leading from increased ROS levels to increased HIF-1α protein levels in PC12 cells subjected to IH.

Materials and Methods

Cell Culture

PC12 cells (original clone from Dr. L. Green) were cultured in Dulbecco's modified Eagle's medium (DMEM) supplemented with 10% horse serum, 5% fetal bovine serum (FBS), penicillin (100 U/ml), and streptomycin (100μg/ml) under 10% CO_2 and 90% air at 37°C. Prior to all experiments, the cells were placed in antibiotic free medium and serum starved for 16 h to avoid any confounding effects of serum on HIF-1 activity. In the experiments involving treatment with drugs, cells were pre-incubated for 30 min with either drug or vehicle.

Exposure to Intermittent Hypoxia

Cell cultures were exposed to IH as described previously (Yuan et al., 2005). Cells were exposed to alternating cycles of 1.5% O_2 for 30 sec followed by 20% O_2 for 5 min at 37°C. Gas flows were controlled by timer-controlled solenoid valves. O_2 levels were monitored by an electrode (Lazar) placed in the tissue culture medium and ambient O_2 levels were monitored by an O_2 analyzer (Beckman LB2).

Chemicals

All chemicals and reagents were of analytical grade and obtained from Sigma Chemical Co. (St. Louis, MO) unless otherwise stated.

Immunoblot Assays

Immunoblot assays were performed as described previously (Yuan et al., 2005). Briefly, cell extracts (25 μg) were fractionated by 7.5% polyacrylamide-SDS gel electrophoresis and transferred to a polyvinylpyrrolidone difluoride membrane (Immobilon-P, Millipore, Bedford, MA). The membrane was blocked with Tris-buffered saline (TBS-T) containing 5% non-fat milk at 4°C overnight. Membranes were incubated with anti-HIF-1α mouse monoclonal antibody H1α67 (Zhong et al., 1999) at 1:500 dilution of stock in TBS-T containing 3% non-fat milk. Membranes were treated with goat anti-mouse secondary antibody conjugated with horseradish peroxidase (Chemicon; dilution 1:2000) in TBS-T containing 3% non-fat milk. Immune complexes on the membrane were visualized using enhanced chemiluminescence (ECL) detection system (Amersham). The membranes were exposed to Kodak XAR films. Similar procedures were employed for immunoblot analysis of: phosphorylated and unphosphorylated forms of phospholipase C (PLCγ), mammalian target of rapamycin (mTOR), and p70 S6 kinase (S6K) (Cell Signaling; dilution 1:1000); phosphorylated forms of protein kinase C (anti-pan $PKC\gamma^{Thr514}$; Cell Signaling; 1:1000 dilution); hydroxylated HIF-1α (gift from Dr. P. Ratcliffe; 1:1000); and tubulin (Sigma; 1:2000).

Transient Transfection and Reporter Gene Assays

Plasmid p2.1 was previously described (Semenza et al., 1996). pRSV-LacZ was obtained from the American Type Culture Collection. Cells were transfected with plasmid DNA using Lipofectamine (Gibco) reagent as previously described (Yuan et al., 2005). Briefly, cells were plated in 35-mm tissue culture plates at a density of 1×10^5 cells/plate in serum containing growth medium. After 24 h, cells were washed twice with 5 ml of serum-free medium. The DNA-liposome mixture was prepared using Lipofectamine (10 μg), 1 μg of p2.1, and 0.25 μg of pRSV-LacZ (internal control for determining the transfection efficiency) in 2 ml of serum-free medium. The total amount of DNA transfected per plate was held constant by addition of pUC19 carrier DNA. Cells were incubated in the DNA-Lipofectamine mixture for 4 h followed by addition of 2 ml of serum-containing medium. After 24 h, cells were washed with serum-free medium and 4 ml of serum-free growth medium was added. After 18 h, cells were exposed to either 20% O_2 or IH and then harvested in 200 μl of lysis buffer. 20 μl of cell lysate was mixed with 100 μl of buffer containing luciferin. Relative luminescent light units were recorded in a Berthold luminometer. β-galactosidase (β-gal) activity was measured using Galacto-Light™ kit (Tropix, Bethesda, MA). Briefly, 10 μl of cell lysate was incubated with 100 μl of the reaction mixture containing β-Galactam™ as substrate for 30 min at room temperature. Following incubation, 150 μl of luminescence enhancer was added to the reaction mixture and the resulting luminescence was measured. Protein analysis was performed using a protein assay kit (BioRad). We verified that all reporter gene assays were in the linear range.

Measurement of intracellular Ca^{2+} ($[Ca^{2+}]_I$)

$[Ca^{2+}]_i$ levels were measured by quantitative fluorescence imaging using the Ca^{2+}-sensitive dye fura 2. Cells plated on collagen coated coverslips were incubated with 3 μM of the fura 2 acetoxymethyl ester (Fura-2 AM; TefLabs) along with 0.06% Pluronic F-127 (Molecular Probes, P-6867) for the last 30 min of IH_{60} exposure. Subsequently, cover slips were viewed under Nikon TE300 inverted microscope and with a cooled charge-coupled device camera under computer control (Metafluor, Universal Imaging). In each experiment, background light levels were determined and subtracted from each image before monitoring the fluorescence intensity ratio at 340 nm/380 nm. $[Ca^{2+}]_i$ was determined by the following equation, $$[Ca^{2+}]_i = K_d * \left[\frac{(R_o - R_{min})}{(R_{max} - R_o)}\right] * \beta$$

where R_o is the measured fluorescence ratio, R_{min} is the fluorescence ratio in the absence of Ca^{2+}, R_{max} is the fluorescence ratio at saturating Ca^{2+}, K_d is the dissociation constant for Fura-2 (224 nM,)and β is the ratio of fluorescence intensity (at 380 nm) in the absence of Ca^{2+} to fluorescence intensity at saturating Ca^{2+} concentrations. Acquisition of image frequency was every 5 sec for 5 min. Data was obtained from at least three independent coverslips in each experimental protocol.

Aconitase activity

Mitochondria were isolated as previously described (Lai and Clark, 1979) except that EDTA was substituted with 1 mM EGTA and the extraction volume was adjusted for smaller sample sizes. Aconitase enzyme activity was determined in the cytosolic and mitochondrial fractions of PC12 cells as previously described (Yuan et al., 2004) and expressed as micromoles of isocitrate per min per mg of protein.

NADPH oxidase activity

The activity of NADPH oxidase was measured as previously described (Mayo and Curnutte, 1990). The reaction was initiated by lysing fresh PC12 cells in HEPES buffer (pH 7.4)

containing 150 μM cytochrome *c*. Absorbance was monitored at 550 nm. The enzyme activity was expressed as nanomoles per min per mg of protein. Reduction of cytochrome *c* was prevented by addition of diphenyl iodonium (3 μM) or apocyanin (1 mM).

Statistical analysis

The data are expressed as mean ± SD from 3–5 independent experiments, each of which was performed in triplicate. Statistical analysis was performed by analysis of variance (ANOVA) and p values < 0.05 were considered significant.

Results

ROS generation by NADPH oxidase is required for HIF-1α accumulation by IH

To assess whether ROS contributes to IH-evoked HIF-1 activation, we first examined the effects of increasing concentrations (25, 50 and 100 μM) of MnTMPyP, a membrane permeable scavenger of $O_2^{\cdot -}$. PC12 cells were transfected with reporter plasmid p2.1, in which the expression of firefly luciferase was driven by a HIF-1-dependent hypoxia response element (HRE) located upstream of a basal SV40 promoter (Semenza et al., 1996). Our previous study showed that HRE-dependent transcriptional activity was induced by 60 cycles of IH (IH_{60}). However, relative to the induction of HIF-1 protein expression, HRE activation by IH_{60} was not as dramatic and required 120 cycles of IH (IH_{120}; Yuan et al., 2005). Therefore, in these experiments, cells were exposed to IH_{120} to determine the effects of MnTMPyP on HIF-1-dependent transcriptional activity. IH_{120} increased HRE activity and this response was blocked by MnTMPyP in a concentration dependent manner, with maximal inhibition occurring at 50 μM (Figure 1A). Based on these results, we analyzed the effect of 50 μM MnTMPyP on HIF-1α protein accumulation in cells subjected to IH. HIF-1α protein levels increased ~4 fold after IH_{60}, whereas HIF-1β protein was unaffected. Pre-treating cells with 50 μM MnTMPyP significantly inhibited IH-evoked HIF-1α accumulation (Figure 1B). To analyze ROS generation, redox-sensitive aconitase enzyme activity was monitored in cytosolic and mitochondrial fractions as an index of $O_2^{\cdot -}$ levels (Gardner et al., 1994). IH_{60} decreased aconitase activity by 61% and 54% in cytosolic and membrane fractions, respectively, an effect that was abolished by MnTMPyP (Figure 1C).

NADPH oxidase (Nox) is a major source of $O_2^{\cdot -}$ generation (Bedard and Krause, 2007). We examined whether IH affects Nox activity and if so, whether Nox activation contributes to IH-evoked HIF-1α accumulation. Nox activity increased 2.5-fold in IH exposed cells, and this effect was abolished by Nox inhibitors apocyanin (1mM; Figure 2A) and 3 μM DPI (data not shown). The increase in Nox activity after IH_{60} was associated with marked increases in the levels of multiple Nox subunit proteins including $gp91^{phox}$, $p22^{phox}$, $p47^{phox}$, and $p67^{phox}$ (Figure 2B). Apocyanin completely prevented HIF-1α accumulation after IH_{60} (Figure 2C). These observations suggest that ROS generation from Nox is required for induction of HIF-1 α protein expression in response to IH.

ROS-dependent Ca^{2+} signaling pathways involving PLCγ and PKC activation are required for IH-evoked HIF-1α accumulation

Ca^{2+} signaling pathways play critical roles in eliciting cellular responses to ROS (Kim et al., 2004; Wang et al., 2006). To assess whether IH increases cytosolic $[Ca^{2+}]$ and, if so, whether it requires Nox-dependent ROS generation, $[Ca^{2+}]_i$ levels were monitored in IH exposed PC12 cells in presence of MnTMPyP or apocyanin. As shown in Fig 3A, IH increased $[Ca^{2+}]_i$ and this effect was blocked by 50μM MnTMPyP or 1 mM apocyanin. Pre-treatment of cells with the intracellular Ca^{2+}-chelator BAPTA-AM prevented IH-induced HIF-1α accumulation in a concentration-dependent manner (Figure 3B), indicating that IH-induced HIF-1α accumulation involves an increase in $[Ca^{2+}]_i$. Elevations in $[Ca^{2+}]_i$ can be

due to Ca^{2+} entry via voltage-dependent Ca^{2+} channels and/or mobilization of intracellular Ca^{2+} stores (e.g., via inositol 1,4,5-trisphosphate [IP3] receptors). Previous studies have shown that nitrendipine, a selective blocker of L-type Ca^{2+} currents inhibits CH elevated $[Ca^{2+}]_i$ and CH augmented voltage-gated Ca^{2+} currents in PC12 cells (Premkumar et al., 2000). However, nitrendipine was ineffective in blocking IH-induced HIF-1α accumulation (Figure 3C), whereas 2-APB, an IP3 receptor inhibitor, blocked the induction of HIF-1α in a concentration-dependent manner (Figure 3D). These observations indicate that mobilization of $[Ca^{2+}]_i$ by IP3 receptor activation is required for HIF-1α accumulation by IH.

IP3 receptor activation requires PLCγ, which is known to be activated by ROS (González-Pacheco et al., 2002). We examined whether IH activates PLCγ, and, if so, whether it requires ROS generation by Nox. To this end, phosphorylated PLCγ (p-PLCγ) levels were monitored as an index of PLCγ activation. IH increased p-PLCγ levels ~3 fold and this response was blocked by 10 μM U73122, a potent inhibitor of PLCγ, but not by 10 μM U73343, an inactive analogue of U73122 (Figure 4A). Pretreatment with MnTMPyP or apocyanin also prevented PLCγ activation by IH (Figure 4A and 4B). More importantly, U73122 but not U73343 inhibited HIF-1α accumulation by IH (Figure 4C) in a concentration-dependent manner (data not shown).

IH activates several PKC isoforms in PC12 cells (Yuan et al., 2005). To examine whether IH-induced PKC activation requires PLCγ, the levels of p-PKCγ$^{Thr\text{-}514}$ were monitored as an index of PKC activation (Cat et al., 2006; Wen et al., 2006). IH increased p-PKC and this effect was abolished by U73122 as well as BAPTA-AM (Figure 5A), suggesting the involvement of PLCγ and Ca^{2+} in PKC activation by IH. In addition, apocyanin and MnTMPyP also blocked phosphorylation of PKC by IH, indicating that activation of Nox and subsequent generation of ROS are upstream signaling events for PKC activation by IH (Figure 5A). Pretreatment of cells with 10μM bisindolylmaleimide-1 (Bis-1), which is an inhibitor of multiple PKC isoforms including α, β_1, β_{11}, γ, δ, and ε isoforms blocked IH-induced increase of HIF-1α (Figure 5B).

IH induced HIF-1α accumulation requires activation of mTOR

We hypothesized that IH-induced HIF-1α accumulation may require PKC-dependent activation of mTOR. To test this possibility, we analyzed the phosphorylation of mTOR at residues 2448 and 2481, which are required for its activation, and of S6K, a direct target of phosphorylation by mTOR. Cells exposed to IH_{60} showed significant increases in mTOR and S6K phosphorylation and these effects were blocked by 100 nM rapamycin, an established inhibitor of mTOR. (Figure 6A and 6B). IH-evoked phosphorylation of mTOR and S6K was also blocked by Bis-1 (PKC inhibitor), U73122 (PLCγ inhibitor), BAPTA-AM (Ca^{2+} chelator), or MnTMPyP ($O_2^{\cdot -}$ scavenger) (Figure 6A and 6B). These observations suggest that IH activates mTOR via ROS-, PLCγ-, and PKC-dependent signaling.

If mTOR activation plays a role in IH induced HIF-1α accumulation, then rapamycin should block the increase in HIF-1α levels after IH_{60}. At concentrations that completely prevented IH-induced mTOR activation, rapamycin only partially inhibited IH-induced HIF-1α accumulation and HIF-1-dependent transcription (Figure 7A and B). These results suggest that the increased accumulation of HIF-1α after IH_{60} is mediated by mTOR-dependent and, possibly, mTOR-independent mechanisms.

IH-evoked HIF-1α accumulation involves both increased synthesis and stability

To determine whether increased protein synthesis contributes to IH-induced HIF-1α accumulation, cells were exposed to IH_{30} and treated with cycloheximide, an inhibitor of protein synthesis, followed by exposure to additional 30 cycles of IH (i.e., a total of IH_{60}).

Parallel experiments were performed wherein cells were treated with vehicle (0.05% ethanol) after IH_{30} instead of cycloheximide. In vehicle treated cells, IH_{60} resulted in greater HIF-1α accumulation than in cycloheximide treated cells. HIF-1α levels in cells exposed to IH_{60} with cycloheximide were similar to those exposed to IH_{30} alone (Figure 8A), suggesting that increased HIF-1α accumulation in the absence of cycloheximide was due at least in part to new synthesis.

In cells exposed to CH, decreased HIF-1α prolyl hydroxylation leads to decreased HIF-1α degradation (Ivan et al., 2001; Jaakkola et al., 2001; Yu et al., 2001). We examined whether IH affects HIF-1α hydroxylation using an antibody that is specific to the hydroxylated form of HIF-1α (HIF-1α-OH). As shown in Figures 8B and 8C, IH-induced HIF-1α accumulation was associated with a marked decrease in HIF-1α-OH levels. ROS inhibitors (MnTMPyP and apocyanin) as well as BAPTA-AM, Bis-1, 2-APB, and U73122 (but not U73343) blocked IH-induced decrease in HIF-1α-OH. These results indicate that HIF-1α degradation is inhibited during IH as a result of prolyl hydroxylase inhibition by ROS-dependent signaling. On the other hand, rapamycin had no effect on IH-evoked decrease in HIF-1α-OH (Figure 8D). Taken together with the effects of cycloheximide (Figure 8A) and the known role of mTOR in promoting HIF-1α protein synthesis (Laughner et al., 2001), these results suggest that the mTOR-dependent increase in HIF-1α reflects increased HIF-1α synthesis, whereas the mTOR-independent effect reflects decreased HIF-1α degradation during IH as a result of decreased prolyl hydroxylation.

IH leads to long-lasting HIF-1α accumulation during re-oxygenation

CH induces increased HIF-1α levels, which return to control levels after several minutes of re-oxygenation (Wang et al., 1995). HIF-1α levels were increased in PC12 cells exposed to CH for 5 h and were markedly reduced after only 10 min of re-oxygenation (Figure 9A). In striking contrast, HIF-1α levels remained significantly elevated after 90 min of re-oxygenation following IH_{60} (Figure 9B). These observations indicate that unlike CH, IH leads to HIF-1α accumulation that persists during re-oxygenation.

To assess whether decreased hydroxylation contributes to persistent HIF-1α during re-oxygenation, hydroxylated (HIF-1α-OH) and total HIF-1α levels were monitored during 90 min of re-oxygenation. HIF-1α-OH levels gradually returned to baseline during re-oxygenation,, yet total HIF-1α levels remained elevated during the entire period of re-oxygenation (Figure 10A), indicating that decreased prolyl hydroxylation does not account for persistent HIF-1 α accumulation during re-oxygenation.

To assess the contribution of protein synthesis, PC12 cells were treated with cycloheximide for the last 30 min prior to completion of the IH_{60} exposure and then were re-oxygenated for 90 min. In cycloheximide treated cells, HIF-1α levels gradually returned to baseline levels during re-oxygenation (Figure 10B). Likewise, treating cells with rapamycin for the last 30 min prior to completion of the IH_{60} exposure also resulted in the decay of HIF-1α levels during re-oxygenation without affecting HIF-1α-OH levels (Figure 10C). These observations suggest that IH leads to long lasting mTOR activation that persists during re-oxygenation. To further test this possibility, phosphorylated mTOR levels were monitored during 90 min of re-oxygenation following IH_{60}. As shown in Figure 11A, phospho-mTOR levels remained elevated during the entire 90 min of re-oxygenation. In striking contrast, CH resulted in modest activation of mTOR, which returned to basal levels within 10 min of re-oxygenation (Figure 11B). From these results we conclude that mTOR-dependent protein synthesis is required for long-lasting elevation of HIF-1α levels during re-oxygenation following IH.

Discussion

In this study, we have delineated signal transduction pathways responsible for the increased levels of HIF-1α protein that are observed when PC12 cells are subjected to IH (Figure 12). Remarkably, IH increased both HIF-1α synthesis and stability via ROS-dependent Ca^{2+} signaling pathways. We have previously demonstrated that increased $[Ca^{+2}]_i$ activates CaMK, which phosphorylates p300 and thereby increases HIF-1 transcriptional activity during IH (Yuan et al., 2005). IH-evoked HIF-1α synthesis and stability are due to increases in ROS generated by Nox activation, which is at least in part due to increased expression of its constituent subunits. The up-regulation of Nox subunits especially $p47^{phox}$ and $p67^{phox}$ in cell cultures by IH is consistent with that reported in the central nervous system of mice exposed to chronic IH (Zhan et al., 2005). Increased levels of ROS have been shown to activate PLCγ (González-Pacheco et al., 2002), which generates IP3 and diacylglycerol (DAG). Treatment of rat cortical astrocytes with hydrogen peroxide was sufficient to induce PLCγ activation and IP3 receptor-dependent increases in $[Ca^{+2}]_i$ (Hong et al., 2006). Consistent with this signaling cascade, IH-evoked HIF-1α accumulation requires ROS-dependent Ca^{2+} signaling pathways involving activation of PLCγ and PKC in PC12 cells.

Increased $[Ca^{+2}]_i$ activates the classical PKC isoforms (PKCα and PKCβ), which in turn activate mTOR, a kinase that promotes HIF-1α protein synthesis (Laughner et al., 2001). Calcium-dependent activation of PKCα and mTOR was reported to induce HIF-1α protein synthesis in PC12 cells exposed to CH for 3 h (Hui et al., 2006). We also found modest mTOR activation by CH. More importantly, our results demonstrate that IH led to robust PKC-dependent activation of mTOR compared to CH. However, an mTOR-dependent increase in HIF-1α protein synthesis contributes to IH-evoked HIF-1α accumulation but rapamycin or cycloheximide treatment resulted in only partial inhibition of IH induced HIF-1α accumulation. Inhibition of prolyl hydroxylase activity leading to HIF-1α stabilization similar to that reported with CH was also observed after IH. The negative regulation of prolyl hydroxylase activity by Ca^{2+}/PLCγ/PKC signaling is a novel finding and further studies are necessary to further elucidate the underlying molecular mechanisms. Taken together, these results indicate that IH-evoked accumulation of HIF-1α reflects both increased synthesis and decreased degradation of protein.

A major difference between CH and IH is the remarkable persistence of elevated HIF-1α protein levels following IH but not CH. mTOR-dependent HIF-1α protein synthesis is responsible for sustaining elevated HIF-1α levels for ($t_{1/2}$ > 90 min) after the cessation of IH compared to the rapid decay ($t_{1/2}$ < 10 min) following CH. The role of mTOR was further supported by its sustained activation during the entire 90 min of re-oxygenation following IH. Although mTOR activation and inhibition of prolyl hydroxylases contribute to HIF-1α accumulation during IH, only mTOR activation is responsible for the persistent elevation of HIF-1α during re-oxygenation, since prolyl hydroxylase activity rapidly returns to control values following re-oxygenation

Sustained induction of HIF-1α and mTOR levels following IH *in vivo* may have important pathophysiological consequences. In mice subjected to chronic IH for 72 cycles per night for 10 days, minute ventilation was significantly increased compared to controls when measured at 2 h, but not at 8 h, after terminating chronic IH (Peng et al., 2006). This phenomenon is known as long term facilitation (LTF) of breathing (Bach and Mitchell, 1996) and involves alterations in carotid body function including induction of sensory LTF (Prabhakar et al., 2005). Remarkably, chronic IH does not induce LTF in rodents treated with the ROS scavenger MnTMPyP (Peng et al., 2003; Peng and Prabhakar, 2003), which blocked IH-induced HIF-1α expression in PC12 cells (Figure 1B) and in mice (Peng, 2006). Furthermore, chronic IH does not induce either LTF of breathing or sensory LTF of the

carotid body in *Hif1a*$^{+/-}$ mice (Peng et al., 2006). Taken together, these results suggest that the persistence of HIF-1α levels following IH may represent a molecular basis underlying LTF of breathing and sensory LTF of the carotid body. Further studies are necessary to determine whether the signal transduction pathway leading to IH-induced HIF-1 activity delineated in PC12 cells (Figure 12) is also responsible for the carotid body-mediated changes in ventilatory and cardiovascular physiology that are observed in chronic IH-exposed rodents and humans experiencing chronic IH as a consequence of recurrent apneas. Finally, due to large fluctuations in tumor microvessel flow rate, cancer cells are also subjected to IH (Kimura et al., 1996), which may activate the same signal transduction pathways that we have delineated in this study.

Acknowledgments

We thank Dr. Peter Ratcliffe for generously providing the antibody against hydroxylated HIF-1α. This work was supported in part by Public Health Service Grants PO1-HL-90554 and RO1-HL-76537 (to NRP) from the National Institutes of Health. The costs of publication of this article were defrayed in part by the payment of page charges.

The abbreviations used are

IH	intermittent hypoxia
CH	Continuous hypoxia
Nox	NADPH oxidase
MnTMPyP	Manganese (III) tetrakis(1-methyl-4-pyridyl) porphyrin pentachloride
CaMK	CaM kinase
HIF	hypoxia-inducible factor
PMSF	phenylmethylsulfonyl fluoride
HRE	hypoxia response element
2-APB	2-amino ethoxydephenyl borate
Bis-1	bisindolylmaleimide 1
PI3K	phosphatidylinositol kinase
PLCγ	phospholipase Cγ
PKC	protein kinase C
IP-3 receptors	inositol 1,4,5-trisphosphate receptors
mTOR	mammalian target of rapamycin

Literature Cited

Ang SO, Chen H, Hirota K, Gordeuk VR, Jelinek J, Guan Y, Liu E, Sergueeva AI, Miasnikova GY, Mole D, Maxwell PH, Stockton DW, Semenza GL, Prchal JT. Disruption of oxygen homeostasis underlies congenital Chuvash polycythemia. Nat Genet. 2002; 32:614–621. [PubMed: 12415268]

Bach KB, Mitchell GS. Hypoxia-induced long-term facilitation of respiratory activity is serotonin dependent. Respir Physiol. 1996; 104:251–260. [PubMed: 8893371]

Bedard K, Krause KH. The NOX family of ROS-generating NADPH oxidases: physiology and pathophysiology. Physiol Rev. 2007; 87:245–313. [PubMed: 17237347]

Cat B, Stuhlmann D, Steinbrenner H, Alili L, Holtkötter O, Sies H, Brenneisen P. Enhancement of tumor invasion depends on transdifferentiation of skin fibroblasts mediated by reactive oxygen species. J Cell Sci. 2006; 119:2727–2738. [PubMed: 16757516]

Coleman ML, Ratcliffe PJ. Oxygen sensing and hypoxia-induced responses. Essays Biochem. 2007; 43:1–15. [PubMed: 17705789]

Gardner PR, Nguyen DD, White CW. Aconitase is a sensitive and critical target of oxygen poisoning in cultured mammalian cells and in rat lungs. Proc Natl Acad Sci USA. 1994; 91:12248–12252. [PubMed: 7991614]

González-Pacheco FR, Caramelo C, Castilla MA, Deudero JJ, Arias J, Yagüe S, Jiménez S, Bragado R, Alvarez-Arroyo MV. Mechanism of vascular smooth muscle cells activation by hydrogen peroxide: role of phospholipase C gamma. Nephrol Dial Transplant. 2002; 17:392–398. [PubMed: 11865083]

Hong JH, Moon SJ, Byun HM, Kim MS, Jo H, Bae YS, Lee SI, Bootman MD, Roderick HL, Shin DM, Seo JT. Critical role of phospholipase Cγ1 in the generation of H_2O_2-evoked $[Ca^{2+}]_i$ oscillations in cultured rat cortical astrocytes. J Biol Chem. 2006; 281:13057–13067. [PubMed: 16543237]

Hui AS, Bauer AL, Striet JB, Schnell PO, Czyzyk-Krzeska MF. Calcium signaling stimulates translation of HIF-α during hypoxia. FASEB J. 2006; 20:466–475. [PubMed: 16507764]

Ivan M, Kondo K, Yang H, Kim W, Valiando J, Ohh M, Salic A, Asara JM, Lane WS, Kaelin WG Jr. HIFα targeted for VHL-mediated destruction by proline hydroxylation: implications for O_2 sensing. Science. 2001; 292:464–468. [PubMed: 11292862]

Iyer NV, Kotch LE, Agani F, Leung SW, Laughner E, Wenger RH, Gassmann M, Gearhart JD, Lawler AM, Yu AY, Semenza GL. Cellular and developmental control of O_2 homeostasis by hypoxia-inducible factor 1α. Genes Dev. 1998; 12:149–162. [PubMed: 9436976]

Jaakkola P, Mole DR, Tian YM, Wilson MI, Gielbert J, Gaskell SJ, Kriegsheim A, Hebestreit HF, Mukherji M, Schofield CJ, Maxwell PH, Pugh CW, Ratcliffe PJ. Targeting of HIF-α to the von Hippel-Lindau ubiquitylation complex by O_2-regulated prolyl hydroxylation. Science. 2001; 292:468–472. [PubMed: 11292861]

Kageyama Y, Koshiji M, To KK, Tian YM, Ratcliffe PJ, Huang LE. Leu-574 of human HIF-1alpha is a molecular determinant of prolyl hydroxylation. FASEB J. 2004; 18:1028–1030. [PubMed: 15084514]

Kim DK, Natarajan N, Prabhakar NR, Kumar GK. Facilitation of dopamine and acetylcholine release by intermittent hypoxia in PC12 cells: involvement of calcium and reactive oxygen species. J Appl Physiol. 2004; 96:1206–1215. [PubMed: 14657041]

Kimura H, Braun RD, Ong ET, Hsu R, Secomb TW, Papahadjopoulos D, Hong K, Dewhirst MW. Fluctuations in red cell flux in tumor microvessels can lead to transient hypoxia and reoxygenation in tumor parenchyma. Cancer Res. 1996; 56:5522–5528. [PubMed: 8968110]

Kline DD, Peng YJ, Manalo DJ, Semenza GL, Prabhakar NR. Defective carotid body function and impaired ventilatory responses to chronic hypoxia in mice partially deficient for hypoxia-inducible factor 1α. Proc Natl Acad Sci USA. 2002; 99:821–826. [PubMed: 11792862]

Kumar GK, Rai V, Sharma SD, Ramakrishnan DP, Peng YJ, Souvannakitti D, Prabhakar NR. Chronic intermittent hypoxia induces hypoxia-evoked catecholamine efflux in adult rat adrenal medulla via oxidative stress. J Physiol. 2006; 575:229–239. [PubMed: 16777938]

Lai JC, Clark JB. Preparation of synaptic and nonsynaptic mitochondria from mammalian brain. Meth Enzymol. 1979; 55:51–60. [PubMed: 459854]

Laughner E, Taghavi P, Chiles K, Mahon PC, Semenza GL. HER2 (neu) signaling increases the rate of hypoxia-inducible factor 1α (HIF-1α) synthesis: novel mechanism for HIF-1-mediated vascular endothelial growth factor expression. Mol Cell Biol. 2001; 21:3995–4004. [PubMed: 11359907]

Mayo LA, Curnutte JT. Kinetic microplate assay for superoxide production by neutrophils and other phagocytic cells. Meth Enzymol. 1990; 186:567–575. [PubMed: 2172715]

Nieto FJ, Young TB, Lind BK, Shahar E, Samet JM, Redline S, D'Agostino RB, Newman AB, Lebowitz MD, Pickering TG. Association of sleep-disordered breathing, sleep apnea, and hypertension in a large community-based study. JAMA. 2000; 283:1829–1836. [PubMed: 10770144]

Peers C. Interactions of chemostimuli at the single cell level: studies in a model system. Exp Physiol. 2004; 89:60–65. [PubMed: 15109210]

Peet DJ, Lando D, Whelan DA, Whitelaw ML, Gorman JJ. Oxygen-dependent asparagine hydroxylation. Methods Enzymol. 2004; 381:467–487. [PubMed: 15063693]

Peng YJ, Overholt JL, Kline D, Kumar GK, Prabhakar NR. Induction of sensory long-term facilitation in the carotid body by intermittent hypoxia: implications for recurrent apneas. Proc Natl Acad Sci USA. 2003; 100:10073–10078. [PubMed: 12907705]

Peng YJ, Prabhakar NR. Reactive oxygen species in the plasticity of respiratory behavior elicited by chronic intermittent hypoxia. J Appl Physiol. 2003; 94:2342–2349. [PubMed: 12533494]

Peng YJ, Yuan G, Ramakrishnan D, Sharma SD, Bosch-Marce M, Kumar GK, Semenza GL, Prabhakar NR. Heterozygous HIF-1α deficiency impairs carotid body-mediated systemic responses and reactive oxygen species generation in mice exposed to intermittent hypoxia. J Physiol. 2006; 577:705–716. [PubMed: 16973705]

Poets CF, Samuels MP, Southall DP. Epidemiology and pathophysiology of apnoea of prematurity. Biol Neonate. 1994; 65:211–219. [PubMed: 8038285]

Prabhakar NR, Peng YJ, Jacono FJ, Kumar GK, Dick TE. Cardiovascular alterations by chronic intermittent hypoxia: importance of carotid body chemoreflexes. Clin Exp Pharmacol Physiol. 2005; 32:447–449. [PubMed: 15854156]

Prabhakar NR, Dick TE, Nanduri J, Kumar GK. Systemic, cellular and molecular analysis of chemoreflex-mediated sympathoexcitation by chronic intermittent hypoxia. Exp Physiol. 2007a; 92:39–44. [PubMed: 17124274]

Prabhakar NR, Kumar GK, Nanduri J, Semenza GL. ROS signaling in systemic and cellular responses to chronic intermittent hypoxia. Antioxid Redox Signal. 2007b; 9:1397–1403. [PubMed: 17627465]

Premkumar DR, Mishra RR, Overholt JL, Simonson MS, Cherniack NS, Prabhakar NR. L-type Ca(2+) channel activation regulates induction of c-fos transcription by hypoxia. J Appl Physiol. 2000; 88:1898–1906. [PubMed: 10797155]

Ramanathan L, Gozal D, Siegel JM. Antioxidant responses to chronic hypoxia in the rat cerebellum and pons. J Neurochem. 2005; 93:47–52. [PubMed: 15773904]

Semenza GL, Jiang BH, Leung SW, Passantino R, Concordet JP, Maire P, Giallongo A. Hypoxia response elements in the aldolase A, enolase 1, and lactate dehydrogenase A gene promoters contain essential binding sites for hypoxia-inducible factor 1. J Biol Chem. 1996; 271:32529–32537. [PubMed: 8955077]

Semenza GL. Oxygen-dependent regulation of mitochondrial respiration by hypoxia-inducible factor 1. Biochem J. 2007; 405:1–9. [PubMed: 17555402]

Shahar E, Whitney CW, Redline S, Lee ET, Newman AB, Nieto J, O'Connor GT, Boland LL, Schwartz JE, Samet JM. Sleep-disordered breathing and cardiovascular disease: cross-sectional results of the sleep heart health study. Am J Respir Crit Care Med. 2001; 163:19–25. [PubMed: 11208620]

Smith TG, Brooks JT, Balanos GM, Lappin TR, Layton DM, Leedham DL, Liu C, Maxwell PH, McMullin MF, McNamara CJ, Percy MJ, Pugh CW, Ratcliffe PJ, Talbot NP, Treacy M, Robbins PA. Mutation of von Hippel-Lindau tumour suppressor and human cardiopulmonary physiology. PLoS Med. 2006; 3:e290. [PubMed: 16768548]

Wang GL, Jiang BH, Rue EA, Semenza GL. Hypoxia-inducible factor 1 is a basic-helix-loop-helix-PAS heterodimer regulated by cellular O_2 tension. Proc Natl Acad Sci USA. 1995; 92:5510–5514. [PubMed: 7539918]

Wang H, Yuan G, Prabhakar NR, Boswell M, Katz DM. Secretion of brain-derived neurotrophic factor from PC12 cells in response to oxidative stress requires autocrine dopamine signaling. J Neurochem. 2006; 96:694–705. [PubMed: 16390493]

Wen Y, Gu J, Li SL, Reddy MA, Natarajan R, Nadler JL. Elevated glucose and diabetes promote interleukin-12 cytokine gene expression in mouse macrophages. Endocrinology. 2006; 147:2518–2525. [PubMed: 16455783]

Yu AY, Shimoda LA, Iyer NV, Huso DL, Sun X, McWilliams R, Beaty T, Sham JS, Weiner CM, Sylvester JT, Semenza GL. Impaired physiological responses to chronic hypoxia in mice partially deficient for hypoxia-inducible factor 1α. J Clin Invest. 1999; 103:691–696. [PubMed: 10074486]

Yu F, White SB, Zhao Q, Lee FS. HIF-1α binding to VHL is regulated by stimulus-sensitive proline hydroxylation. Proc Natl Acad Sci USA. 2001; 98:9630–9635. [PubMed: 11504942]

Yuan G, Adhikary G, McCormick AA, Holcroft JJ, Kumar GK, Prabhakar NR. Role of oxidative stress in intermittent hypoxia-induced immediate early gene activation in rat PC12 cells. J Physiol. 2004; 557:773–783. [PubMed: 15107478]

Yuan G, Nanduri J, Bhasker CR, Semenza GL, Prabhakar NR. Ca^{2+}/calmodulin kinase-dependent activation of hypoxia inducible factor 1 transcriptional activity in cells subjected to intermittent hypoxia. J Biol Chem. 2005; 280:4321–4328. [PubMed: 15569687]

Zhan G, Serrano F, Fenik P, Hsu R, Kong L, Pratico D, Klann E, Veasey SC. NADPH oxidase mediates hypersomnolence and brain oxidative injury in a murine model of sleep apnea. Am J Respir Crit Care Med. 2005; 172:921–929. [PubMed: 15994465]

Zhong H, De Marzo AM, Laughner E, Lim M, Hilton DA, Zagzag D, Buechler P, Isaacs WB, Semenza GL, Simons JW. Overexpression of hypoxia-inducible factor 1α in common human cancers and their metastases. Cancer Res. 1999; 59:5830–5835. [PubMed: 10582706]

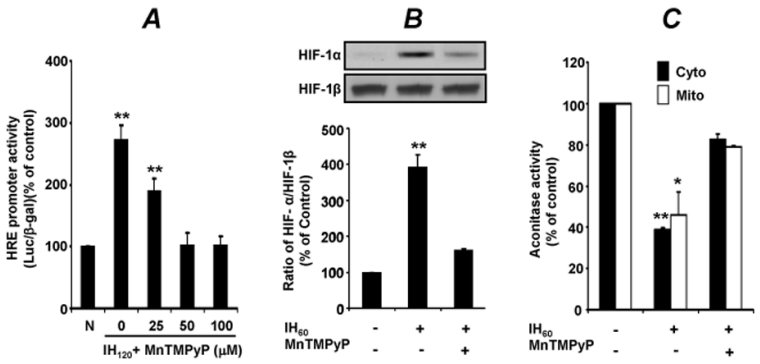

Fig. 1. Involvement of ROS in IH-evoked accumulation of HIF-1α

(A) PC12 cells were co-transfected with p2.1, which contains a hypoxia response element upstream of SV40 promoter and luciferase coding sequences, and pRSV-LacZ, which contains RSV promoter and β-galactosidase coding sequences. Transfected cells were exposed to either normoxia (N) or to 120 cycles of IH (IH_{120}) in the presence of increasing concentrations of ROS scavenger MnTMPyP. (B) HIF-1α and HIF-1β proteins were analyzed by immunoblot assay in cells exposed to normoxia or 60 cycles of IH (IH_{60}) in the presence or absence of MnTMPyP (50 μM). *Top panel*: representative western blots; *Bottom panel:* densitometric analysis. Data presented are mean ± S.D. from 3 independent experiments. (C) Aconitase enzyme activity was determined in cytosolic and mitochondrial fractions as an index of ROS generation in PC12 cells exposed to IH_{60} in the presence or absence of MnTMPyP (50 μM). Data presented are mean ± S.D. from three independent experiments. ** $p < 0.01$, * $p < 0.05$ compared with control.

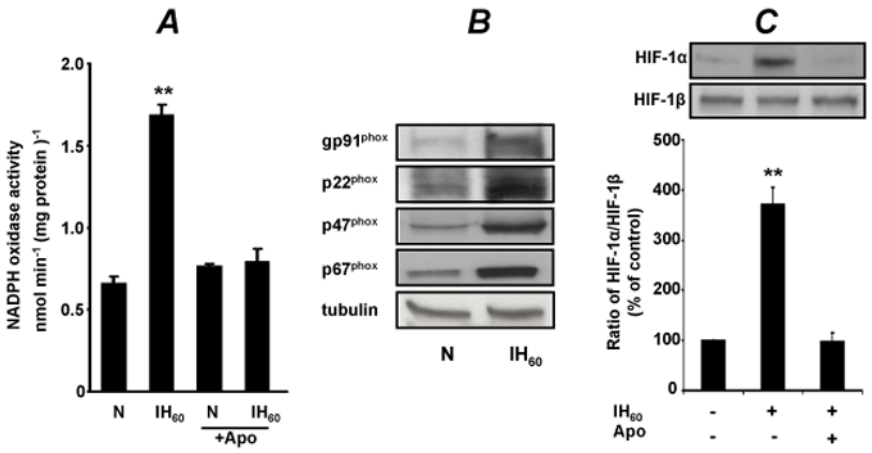

Fig. 2. Activation of NADPH oxidase by IH

(A) NADPH oxidase activity was determined in cells exposed to normoxia (N) or to IH_{60} in the absence or presence of 1 mM apocyanin (Apo), an NADPH oxidase inhibitor. (B) Representative immunoblot showing the effect of IH on NADPH oxidase subunit protein levels ($gp91^{phox}$, $p22^{phox}$, $p47^{phox}$, and $p67^{phox}$). (C) HIF-1α and HIF-1β protein levels were determined in lysates from control and IH_{60} exposed cells in the presence (+) or absence (−) of apocyanin (Apo; 1 mM). *Top panel*: representative immunoblots. *Bottom panel*: densitometric analysis. Data presented are mean ± S.D. from 3–5 independent experiments. **p< 0.01 compared with control.

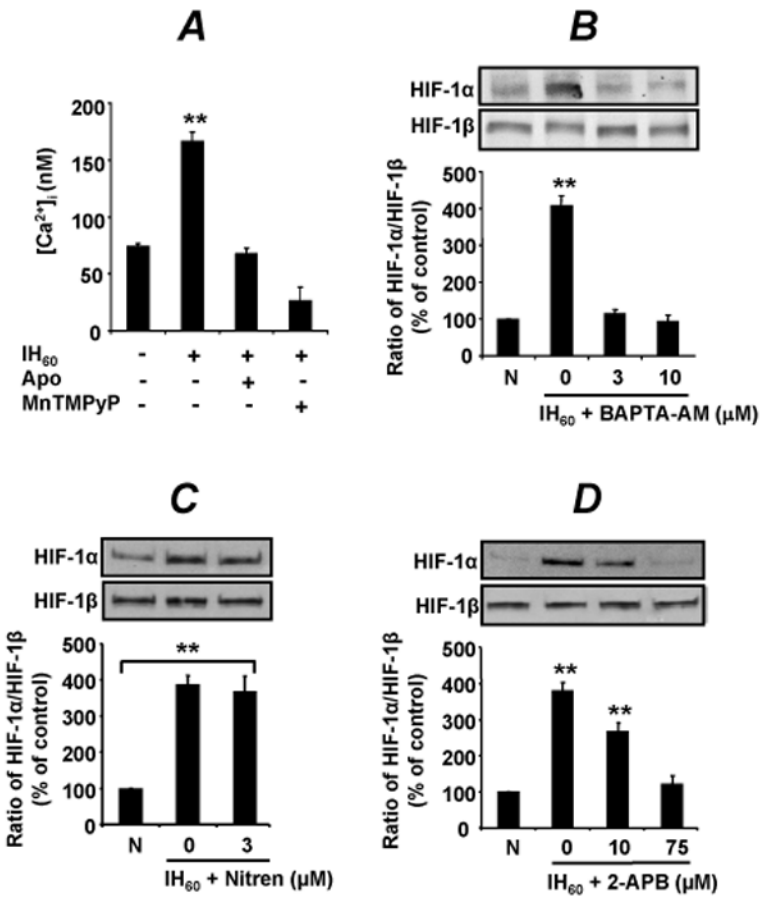

Fig. 3. Increased intracellular Ca^{2+} contributes to IH-induced HIF-1α accumulation

(**A**) $[Ca^{2+}]_i$ levels were monitored by Fura-2 AM using fluorescence imaging in PC12 cells exposed to IH_{60} in presence of 1 mM apocyaninor 50 μM MnTMPyP. (**B–D**) Cells were exposed to normoxia (N) or IH_{60} after pretreatment with the indicated concentration of BAPTA-AM, a Ca^{2+} chelator (**B)**; nitrendipine (Nitren), an L-type Ca^{2+} channel blocker (**C**); or 2-APB, an IP-3 receptor blocker (**D**). *Top panels*: representative immunoblots of HIF-1α and HIF-1β protein. *Bottom panels:* densitometric analysis. Data presented are mean ± S.D. from three independent experiments. ** $p< 0.01$, * $p< 0.05$.

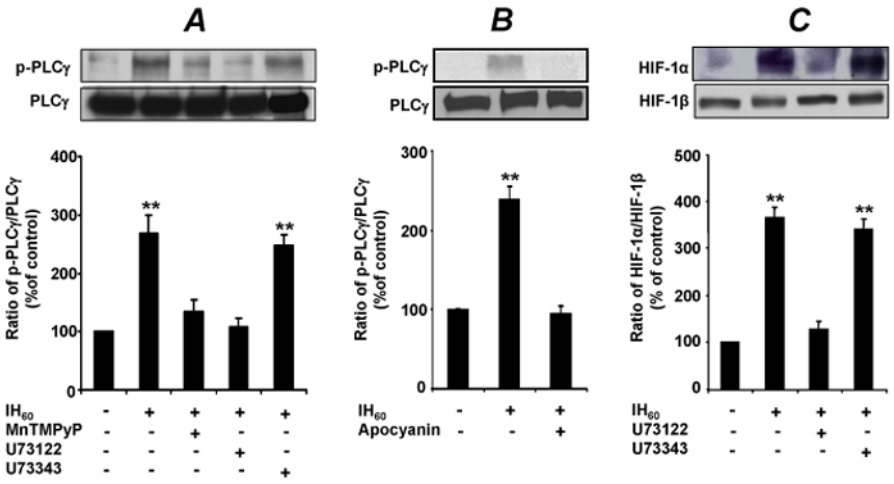

Fig. 4. Activation of PLCγ by IH

(**A–B**) Phosphorylated PLCγ levels (p-PLCγ) were determined by immunoblot assay in cells exposed to nomoxia (−) or IH_{60} (+) pretreated with 50 μM MnTMPyP, 10 μM U73122 (a PLCγ inhibitor), 10 μM U73343 (an inactive analogue of U73122) (**A)**, or 1 mM apocyanin (**B**). PLCγ= total PLCγ. (**C**) Effect of U73122 and U73343 on IH_{60} evoked HIF-1α accumulation. *Top panels*: representative immunoblots of HIF-1α and HIF-1β protein. *Bottom panels*: densitometric analysis. Data presented are mean ± S.D. from three independent experiments. ** $p < 0.01$.

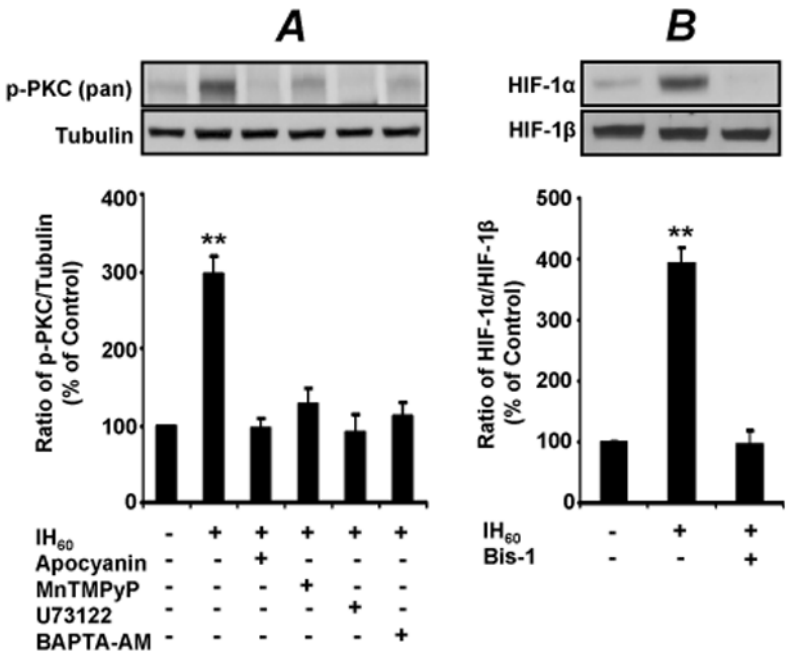

Fig. 5. Involvement of PKC in IH-induced accumulation of HIF-1α

(A) Phosphorylation of PKC was analyzed by immunoblots in cells exposed to normoxia (−) IH_{60} (+) in presence or absence of apocyanin (1 mM), MnTMPyP (50 μM), U73122 (10 μM), or BAPTA-AM (10 μM). (**B**) Effect of 10μM Bis-1, a PKC inhibitor on HIF-1α and HIF-1β proteins. *Top panels*: representative immunoblots. *Bottom panels*: densitometric analysis. Data presented are mean ± S.D. from three independent experiments. **p< 0.01.

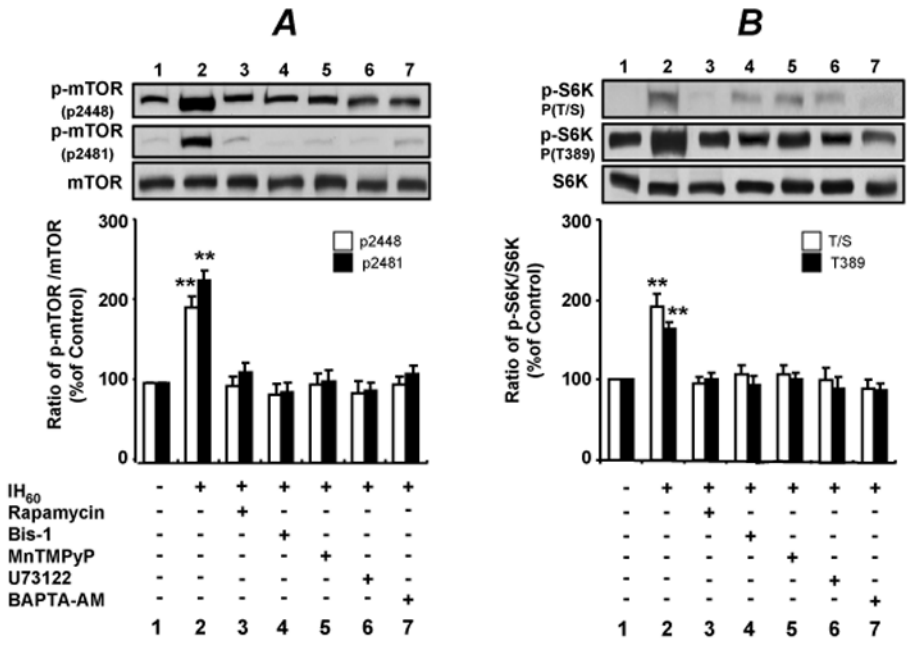

Fig. 6. IH activates mTOR and S6 kinase

(A) Phosphorylation of mTOR was analyzed in PC12 cells exposed to normoxia (−) or to IH_{60} (+) pretreated with 100 nM rapamycin (an inhibitor of mTOR), 10 μM Bis-1, 50 μM MnTMPyP, 10 μM U73122, 75 μM 2-APB or 10 μM BAPTA-AM as indicated in lanes 1–7. (**B**) Phosphorylation of S6 kinase was analyzed in the same samples. *Top panels*: representative immunoblots. *Bottom panels*: densitometric analysis. Data presented are mean ± S.D. from three independent experiments. **p< 0.01.

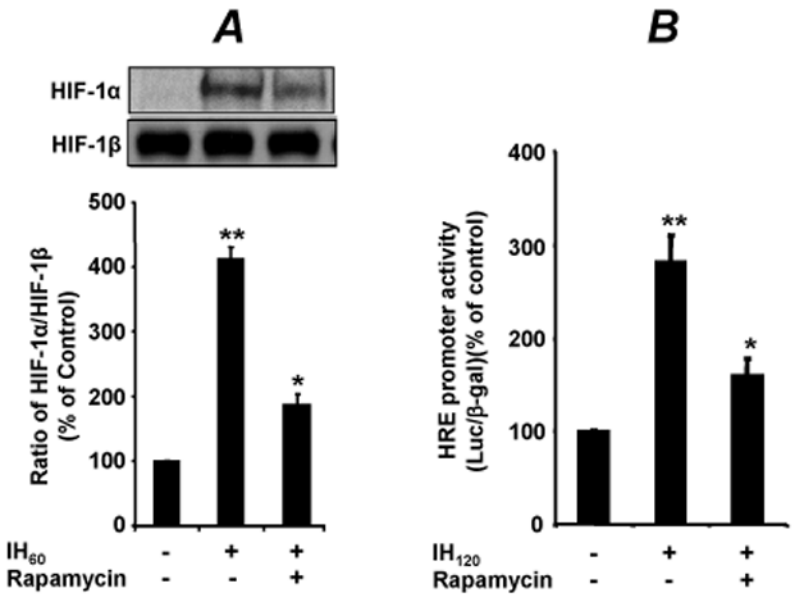

Fig. 7. Rapamycin partially inhibits IH-induced accumulation of HIF-1α

(A) Effect of 100nM rapamycin on HIF-1α and HIF-1β in cell lysates exposed to normoxia (−) or to IH_{60} (+). *Top panel*: representative immunoblots. *Bottom panel*: densitometric analysis. (**B**) Effect of 100 nM rapamycin on HRE-dependent transcription in cells co-transfected with reporter genes p2.1 and pRSV-LacZ and exposed to either normoxia (−) or IH_{120} (+). Data represent mean ± S.D. from three independent experiments. ** $p < 0.01$, * $p < 0.05$.

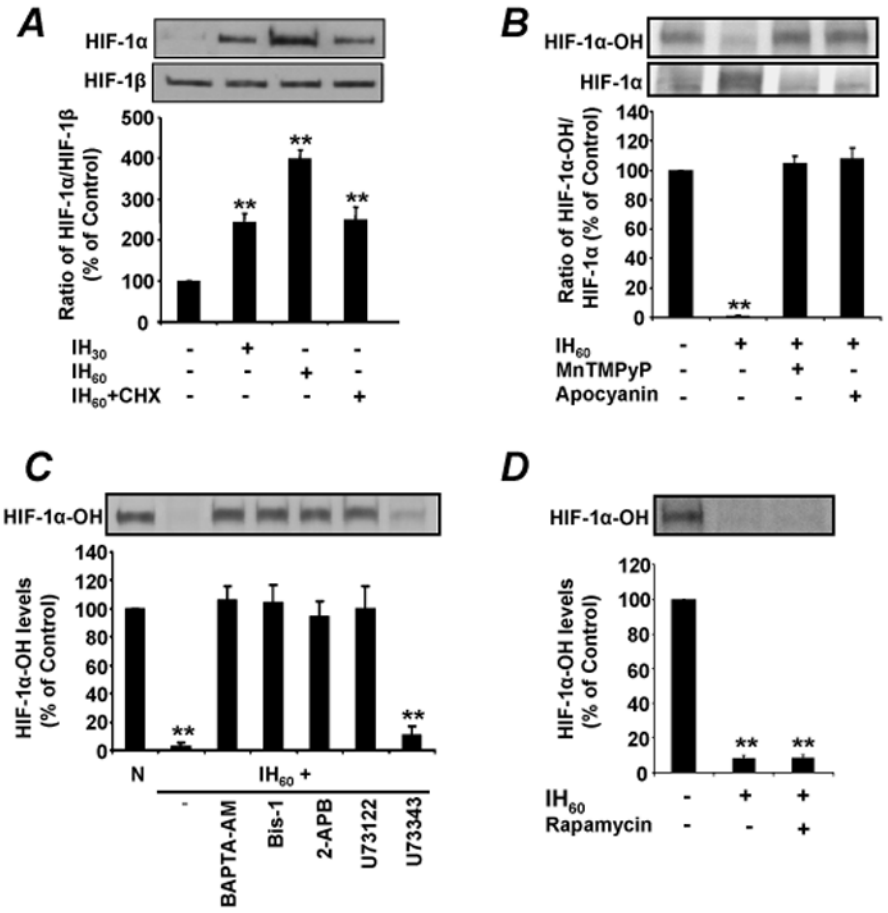

Fig. 8. Increased synthesis and decreased hydroxylation of HIF-1α during IH

(**A**) Effect of cycloheximide on IH-evoked HIF-1α accumulation. Cells were exposed to IH_{60} in presence of vehicle or cycloheximide (20 nM) added after IH_{30}. (**B**) Effect of 50 μM MnTMPyP or 1 mM apocyanin on hydroxylated HIF-1α (HIF-1α-OH) levels. (**C**) Effect of 10 μM BAPTA-AM, 10 μM Bis-1, 75 μM 2-APB, 10 μM U73122, or 10 μM U73343 on HIF-1α-OH levels. (**D**) Effect of 100 nM rapamycin on HIF-1α accumulation and hydroxylation. *Top panels*: representative immunoblots. *Bottom panels*: densitometric analysis. Data presented are mean ± S.D. from three individual experiments. ** $p < 0.01$.

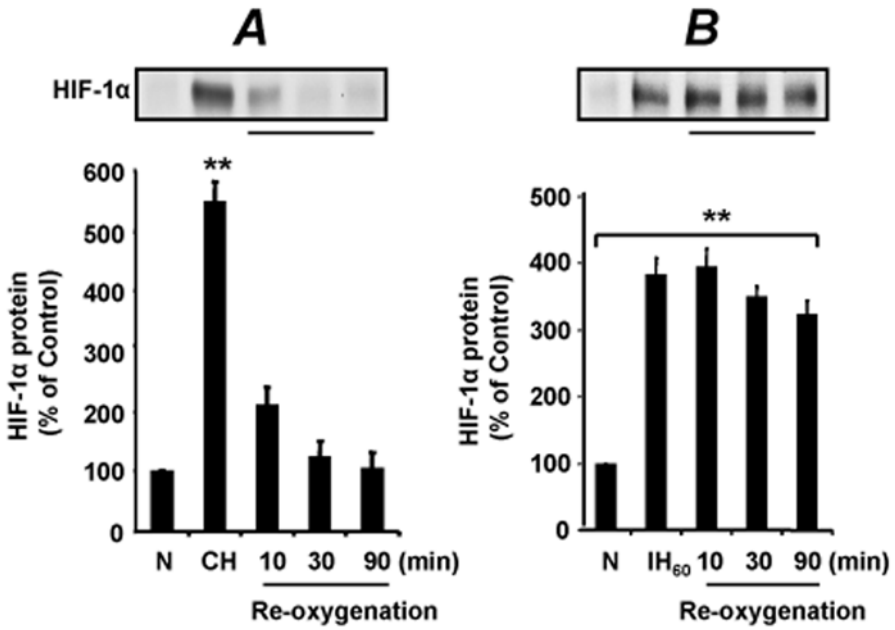

Fig. 9. IH-induced HIF-1α accumulation persists during re-oxygenation

(**A–B**) PC12 cells were exposed to 5 h of continuous hypoxia (CH; **A**) or to IH_{60} (B) followed by 90 min of re-oxygenation (**B**). HIF-1α protein was analyzed by immunoblots. *Top panels*: representative immunoblots. *Bottom panels*: densitometric analysis. Data presented are mean ± S.D. from three independent experiments. **p< 0.01.

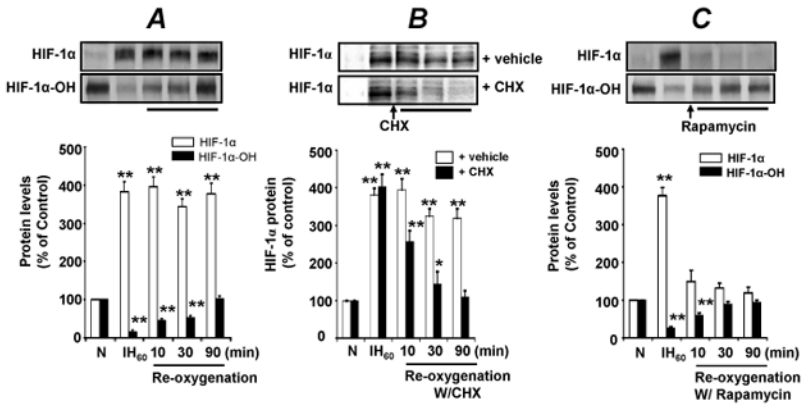

Fig. 10. Protein synthesis and mTOR are required for persistent HIF-1α levels following re-oxygenation

(A) Analysis of HIF-1α and HIF-1α-OH in PC12 cells subjected to IH followed by 90 min re-oxygenation. (B) Effect of 20 nM cycloheximide on HIF-1α levels during re-oxygenation and (C) Effect of 100 nM rapamycin on HIF-1α and HIF-1α-OH levels during re-oxygenation. Cycloheximide and rapamycin were added 30 min prior to the completion of IH exposure. *Top panels*: representative immunoblots. *Bottom panels*: densitometric analysis. Data presented are mean ± S.D. from three independent experiments. **p < 0.01.

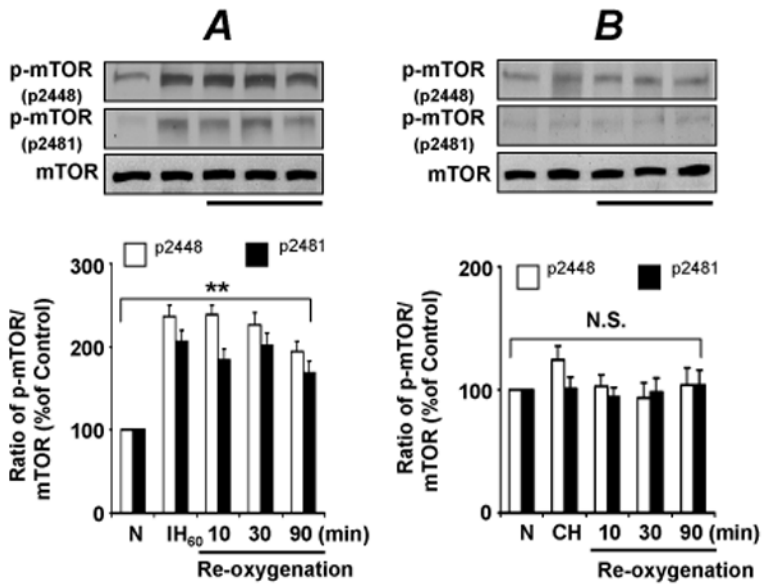

Fig. 11. IH-induced mTOR activation persists during re-oxygenation. Levels of phosphorylated mTOR were determined in cells subjected to IH_{60} followed by 0–90 min of re-oxygenation (**A**) and in cells subjected to 3 h of continuous hypoxia (CH) followed by 0–90 min of re-oxygenation (**B**). mTOR proteins were analyzed by immunoblot assay. *Top panels*: representative immunoblots. *Bottom panels*: densitometric analysis. Data presented are mean ± S.D. from three independent experiments. **p< 0.01.

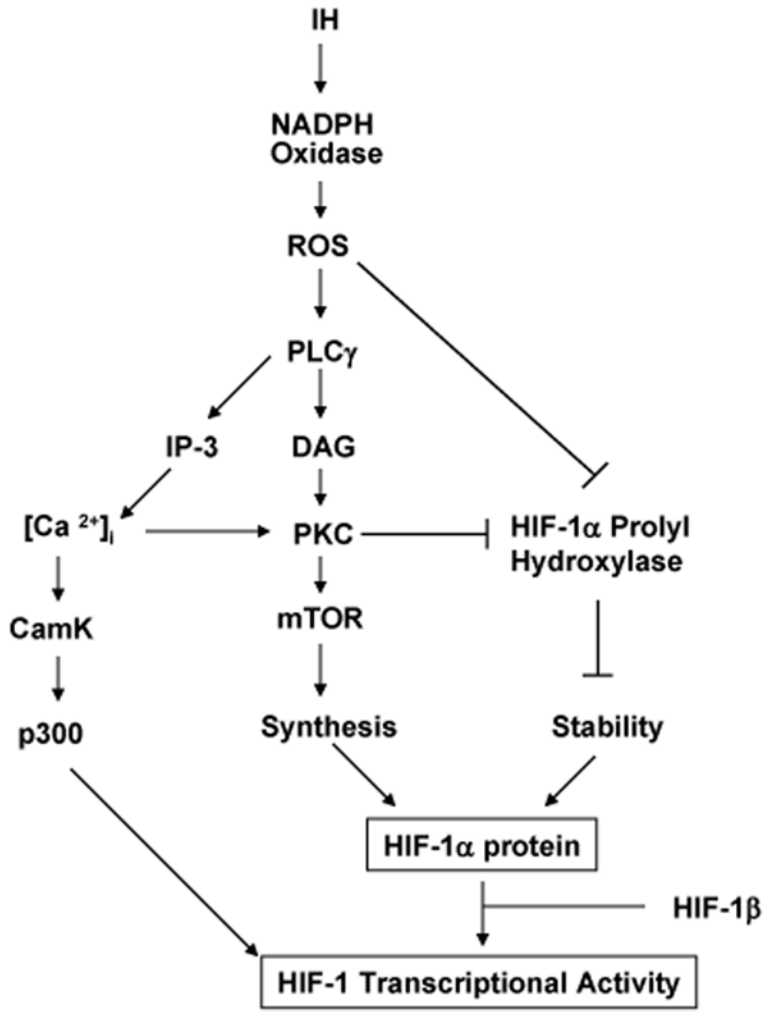

Fig. 12. Signal transduction pathways involved in IH-induced HIF-1α protein expression and HIF-1 transcriptional activity

IH-induced HIF-1α protein expression results from mTOR-dependent increased synthesis and decreased prolyl hydroxylation, which are mediated by ROS-dependent Ca^{2+} signaling pathways. Induction of HIF-1α trans-activation function by IH requires ROS-mediated Ca^{2+}/calmodulin kinase (CaMK)-dependent phosphorylation of the co-activator p300, as reported previously (Yuan et al. 2005).